Study of Adsorption and Decomposition of H_2O on Ge(100)

Soon Jung Jung,[†] Jun Young Lee,[†] Suklyun Hong,*[,‡] and Sehun Kim*[,†]

Department of Chemistry and School of Molecular Science (BK 21), Korea Advanced Institute of Science and Technology, Daejeon 305-701, Republic of Korea, and Department of Physics and Institute of Fundamental Physics, Sejong University, Seoul 143-747, Republic of Korea

Received: August 8, 2005; In Final Form: October 9, 2005

The adsorption and decomposition of water on Ge(100) have been investigated using real-time scanning tunneling microscopy (STM) and density-functional theory (DFT) calculations. The STM results revealed two distinct adsorption features of H_2O on Ge(100) corresponding to molecular adsorption and H−OH dissociative adsorption. In the molecular adsorption geometry, H_2O molecules are bound to the surface via Ge−O dative bonds between the O atom of H_2O and the electrophillic down atom of the Ge dimer. In the dissociative adsorption geometry, the H_2O molecule dissociates into H and OH, which bind covalently to a Ge−Ge dimer on Ge(100) in an H−Ge−Ge−OH configuration. The DFT calculations showed that the dissociative adsorption geometry is more stable than the molecular adsorption geometry. This finding is consistent with the STM results, which showed that the dissociative product becomes dominant as the H_2O coverage is increased. The simulated STM images agreed very well with the experimental images. In the real-time STM experiments, we also observed a structural transformation of the H_2O molecule from the molecular adsorption to the dissociative adsorption geometry.

Introduction

The oxidation of semiconductor surfaces has drawn intense interest on account of the technological importance of oxide films[1,2] as insulating layers in microelectronic devices. The development of semiconductor-based resonant tunneling diodes and smaller transistors has led to the need for uniform, thin, and smooth oxide films. In addition, the interaction between the semiconductor surface and water has received considerable attention due to the widespread use of water in industrial oxidation processes.[3−10]

The adsorption of H_2O on Si surfaces has been studied by various research groups. The adsorption structure of H_2O on a Si(100) surface is a subject of controversy, although recent investigations have consistently indicated that H_2O adsorbs dissociatively on the Si(100) surface at room temperature.[11−18] Despite the similarities between Si(100) and Ge(100), the adsorption behavior of H_2O on Si(100) is expected to be quite different from that on Ge(100) due to subtle differences in the chemical reactivities of these surfaces. The sticking probability of H_2O on Ge(100) is lower than that on Si(100),[19] indicating that it is more difficult for H_2O to adsorb on the Ge surface. Previous studies of the H_2O/Ge(100) system did not report the adsorption structure of H_2O on Ge(100) at room temperature.[20−25]

In the present study, we examined the adsorption geometries of H_2O adsorbed on a Ge(100) surface at room temperature using a combination of scanning tunneling microscopy (STM) and density-functional theory (DFT) calculations. We also observed a structural transformation of the H_2O molecule from the molecular adsorption to the dissociative adsorption geometry.

* Corresponding authors. E-mail: sehun-kim@kaist.ac.kr (S.K.); hong@sejong.ac.kr (S.H.).
[†] Korea Advanced Institute of Science and Technology.
[‡] Sejong University.

Experimental and Theoretical Methods

Experimental Details. The experiments were performed in an ultrahigh-vacuum (UHV) chamber (base pressure $<2.0 \times 10^{-10}$ Torr) equipped with an Omicron VT-STM instrument. A Ge(100) sample (p-type, $\rho = 0.10-0.39\ \Omega$) was cleaved to a size of 2×10 mm^2 and mounted between two tantalum foil clips for the STM measurements. The Ge(100) surface was cleaned using several cycles of sputtering with 1 keV Ar^+ ions for 20 min at 700 K, followed by annealing at 900 K for 10 min. The cleanliness of the Ge(100)-2×1 surface was checked with STM. An infrared optical pyrometer was used to measure the Ge(100) sample temperature. Water (H_2O, deionized) was further purified by several freeze−pump−thaw cycles to remove all dissolved gases prior to dosing. The purity of the water was checked using mass spectrometry. Water was introduced into the UHV chamber through a doser with a seven-capillary array controlled by a variable leak valve at room temperature. All STM images were recorded at a sample voltage between $V_s = -2.0$ and $+2.0$ V with a tunneling current of $I_t = 0.1$ nA using electrochemically etched W-tips.

Theoretical Calculations. Ab initio calculations were performed within the generalized gradient approximation (GGA) using the Vienna ab initio simulation package (VASP).[26] The atoms were represented by ultrasoft pseudopotentials,[27] as provided by VASP, and a kinetic energy cutoff of 270 eV was chosen. The water-adsorbed Ge(100) surface was modeled as a slab composed of water molecules, six Ge layers, and an H layer passivating the bottom surface. The positions of the atoms in the two bottom Ge layers and the H layer were fixed, while the other layers were relaxed with residual forces smaller than 0.02 eV/Å. Gaussian broadening with a width of 0.02 eV was used to accelerate the convergence in the *k*-point sum. With the use of self-consistent Kohn−Sham eigenvalues and wave functions, the constant-current STM images were simulated using the Tersoff−Hamann scheme.[28]

10.1021/jp054415o CCC: $30.25
Published on Web 12/01/2005

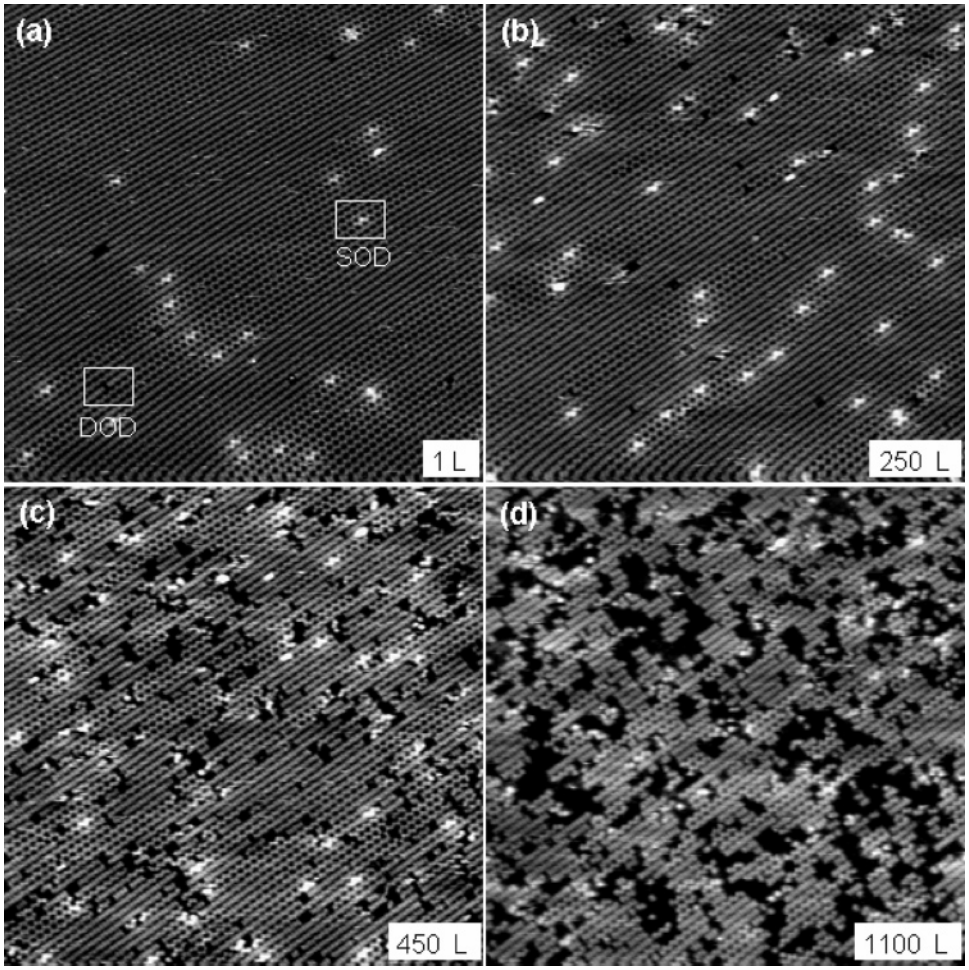

Figure 1. Filled-state STM images (50×50 nm^2, $V_s = -1.6$ V, $I_t = 0.2$ nA) of the Ge(100) surface after exposure to (a) 1.0 L, (b) 250 L, (c) 450 L, and (d) 1100 L of H_2O. (SOD, singly occupied dimer; DOD, doubly occupied dimer.)

Results and Discussion

Figure 1a−d shows a series of filled-state ($V_s = -2.0$ V) STM images recorded in real time during the exposure of the Ge(100) surface to H_2O. The surface atoms and dimers are well resolved. All four images were recorded over the same area. Two distinct features, bright protrusions and dark depressions, are observed in the STM images. As the H_2O exposure is increased, the number of dark features is increased. The coverage of H_2O on Ge(100) was only 0.2 ML even after the exposure of 1000 L (1 langmuir $= 1.33 \times 10^{-6}$ mbar s) of H_2O to the surface, indicating the low sticking probability of H_2O on Ge(100).

We frequently observed structural changes of the H_2O-adsorbed Ge(100) surface after exposure of the surface to 300 L of H_2O while recording STM images for the same area, as shown in Figure 2a,b. For example, the magnified images shown in the left corners of Figure 2a,b reveal that a bright protrusion in Figure 2a transforms into a dark feature in Figure 2b. We carefully investigated the structural change of the Ge(100) surface during adsorption of H_2O and the transition from bright protrusion to dark feature. The bright protrusions appeared to be structures with an H_2O molecule adsorbed molecularly on one side of a Ge dimer; hence these structures are referred to as singly occupied dimers (SODs) (Figure 3a). We also examined various possibilities for the darker image. The possibilities are the extraction of an up-Ge atom, the passivation by a free water molecule, or the dissociation of a datively bonded water molecule. The extraction of an up-Ge atom from the surface by a water molecule seems to be impossible at room temperature due to the high bond energy between Ge atoms. The passivation of the remaining Ge atom in an already water-adsorbed Ge dimer by a free H_2O molecule is unlikely because both the oxygen of the free H_2O and the up-Ge atom of the dimer are electron-rich atoms. We proposed the formation of the dark feature via dissociation of the datively bonded H_2O molecule. The dark features are made up of H and OH, formed by the dissociation of an H_2O molecule, bound to a Ge dimer, with the H bound to one Ge of the dimer and the OH to the

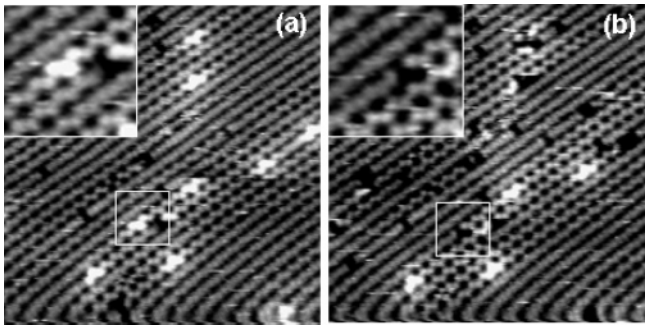

Figure 2. Sequential STM images (20×20 nm^2, $V_s = -1.6$ V, $I_t = 0.2$ nA) of the same region showing the structure transformation of the H_2O-adsorbed Ge(100) surface. SODs attributed to the adsorption of water are shown in (a), which are transformed to DODs in (b). The areas enclosed with white boxes (4×4 nm^2) are enlarged in the upper left of the images.

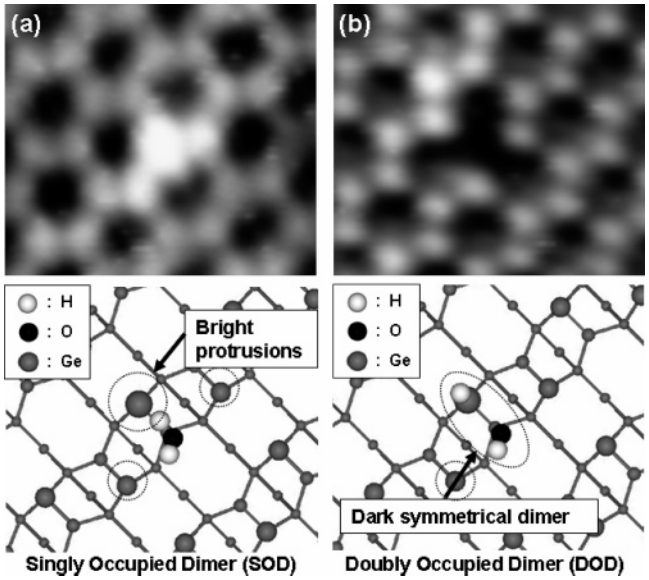

Figure 3. Filled-state STM images (4×3.5 nm^2, $V_s = -1.6$ V, $I_t = 0.2$ nA) and structural diagrams showing (a) SODs and (b) DODs.

other; hence these features are referred to as doubly occupied dimmers (DODs) (Figure 3b).

The number of SODs remained approximately constant with increasing dosing time because some of them were desorbed and others changed to DODs. By contrast, the number of DODs increased in proportion to the dosing time because the DODs are too stable to desorb or change to another structure. The STM results thus show that the DODs accumulate with dosing time but the SODs do not. We would note that although the density of SODs on the surface is approximately independent of the dosing time, it depends on the flux.

Figure 4a−c shows filled-state STM images of the Ge(100) surface recorded after dosing the same surface region with 1100 L of H_2O at room temperature at surface bias voltages of $V_s = -1.6$, -1.2, and -0.8 V, respectively. The STM images of the H_2O-adsorbed surface recorded at different bias voltages are markedly different from each other, indicating a dependence on bias voltage similar to that found previously for the STM images of pyridine on Ge(100).[29] Specifically, the STM image recorded at $V_s = -1.6$ V (Figure 4a) shows dark features associated with DODs and some bright features associated with SODs. At the lower bias voltage of $V_s = -1.2$ V (Figure 4b), the dark feature attributed to DODs in Figure 4a becomes lighter. In the image at the bias voltage of $V_s = -0.8$ V (Figure 4c), the dark features attributed to DODs in Figure 4a are clearly imaged as two well-separated protrusions positioned at the dimers, indicating that each protrusion is associated with each Ge atom of the dimer that reacted with H_2O. The Ge dimers that have reacted with H_2O look different from the bare Ge dimer with π-bonding characteristics, since the bare dimer is imaged as a single oval-shaped protrusion. It is thus concluded that the reaction of H_2O with the Ge dimer, which binds covalently to a Ge−Ge dimer on Ge(100) in an H−Ge−Ge−OH configuration, is likely to break the Ge−Ge π bond to form Ge−H and Ge−OH bonds, resulting in two separate protrusions on the STM image recorded at $V_s = -0.8$ V. It is worthwhile to note that at $V_s = -1.2$ V, even the difference in brightness between two protrusions at the same dimer is seen, and some of the DODs are shown as just one protrusion with the other being dark. These image elements can be attributed to the difference in electron density between Ge−H and Ge−OH.

To determine the atomic-level adsorption geometries of H_2O on Ge(100), we performed ab initio calculations for many possible adsorption configurations. Among the possible configurations, the most stable geometry for molecular adsorption of H_2O on Ge(100) was found to be that arising when H_2O adsorbs molecularly on Ge(100) via formation of a Ge−O dative bond between the O atom of water and the electrophilic down-Ge atom of the Ge dimer, as shown in Figure 5a. For the lowest energy configuration, we calculated the adsorption energy, E_{ad}, defined as

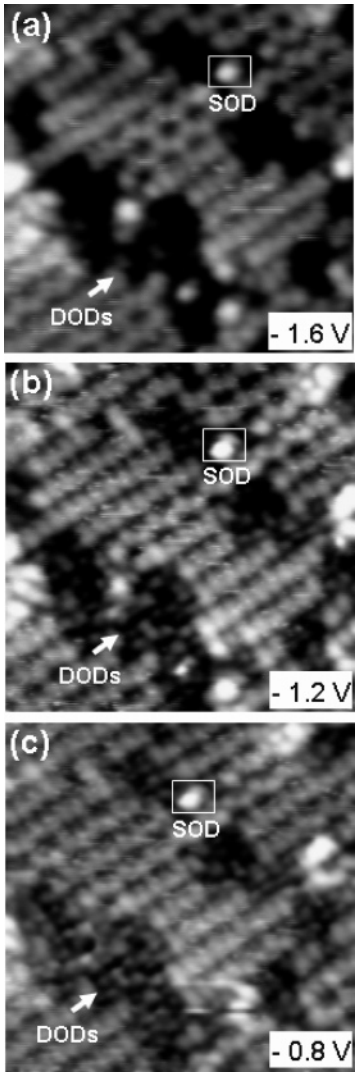

Figure 4. STM images (10×10 nm^2, $I_t = 0.1$ nA) of H_2O on Ge(100) at bias voltages of (a) $V_s = -1.6$ V, (b) -1.2 V, and (c) -0.8 V.

$$E_{ad} = -[E_{tot}(\text{adsorbed}) - E_{tot}(\text{clean}) - E(H_2O)]$$

where E_{tot}(adsorbed), E_{tot}(clean), and $E(H_2O)$ are the total energies of the H_2O-adsorbed surface, the clean $p(2 \times 2)$ surface, and the free water molecule, respectively. The adsorption energy of this configuration in a $p(2 \times 2)$ unit cell is 0.74 eV, compared with the previous result (0.33 eV).[22] Note that the buckling angle of the dimer on the clean Ge(100) surface with $p(2 \times 2)$ symmetry is found to be about 20°. The corresponding values by Kruger and Pollmann[30] and Needels et al.[31] are 19° and 14°, respectively. After adsorption of the water molecule, the up-Ge atom remains in the buckled-up state, but the buckling angle decreases to about 16°. For the optimized geometry, we simulated the filled-state STM image at a bias voltage of $V_s = -1.6$ V (Figure 5a). In the simulated image, the up-Ge atom of

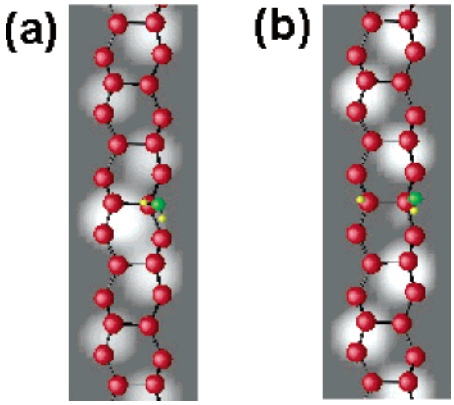

Figure 5. Theoretically calculated filled-state (−1.6 V) STM images: (a) a water molecule adsorbed on a Ge(100) surface and (b) dissociated H and OH on Ge(100). The top view of the surface is superimposed on each simulated image.

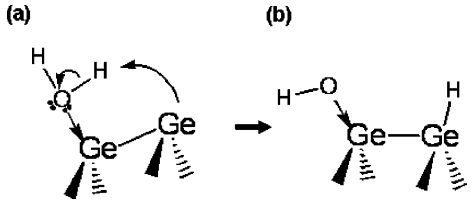

Figure 6. Schematic illustration of the surface reactions between an H_2O molecule and the Ge(100) surface.

the Ge dimer that reacts with H_2O appears brighter than the up atoms of the neighboring dimers. [To simulate the exact features shown in the experimental STM images, we used a larger surface unit cell of $p(2 \times 4)$ in generating Figure 5a,b.] By contrast, the down-Ge atom to which H_2O bonds datively appears as dark as the other down-Ge atoms of the dimer row. The simulated STM image is in good agreement with the experimental STM image shown in Figure 3a.

On the other hand, among the possible dissociative adsorption geometries, the most stable configuration is that in which H_2O adsorbs dissociatively to form an H−Ge−Ge−OH configuration on the Ge(100) surface. In this case, the Ge dimers with H and OH attached become almost symmetric due to a redistribution of the electronic charge. The adsorption energy of this dissociative configuration is 1.32 eV, which is 0.58 eV more stable than the molecular adsorption configuration. Our value (1.32 eV) is compared with the previous one (1.06 eV).[22] The simulated STM image of this configuration (Figure 5b) agrees very well with the experimental image (Figure 3b).

Based on the STM experiment and DFT calculations, we can propose a reasonable adsorption mechanism as illustrated in Figure 6. The oxygen atom of each H_2O molecule contains lone pairs of electrons that can interact with the electrophilic down atom of a buckled dimer to form a dative bond via Lewis acid−base reaction, as illustrated in Figure 6a. Upon initial adsorption of the H_2O, the up atom of the dimer, being electron rich, can act as a nucleophilic surface site. Then, after O−H dissociation, the nucleophilic up atom may attract the dissociated proton (hydrogen) of the H_2O molecule. The final surface configuration after dissociation, in which the dimer becomes almost symmetric due to charge redistribution, is shown in Figure 6b. This reaction is similar to the dissociative adsorption of amines,[32−38] a reaction which has been well documented by various groups.

The energy barrier for the dissociation of H_2O is larger on Ge(100) than on Si(100), but the adsorption energy of H_2O on Ge(100) is smaller than that on Si(100).[20−22] The higher activation energy for O−H dissociation on the Ge(100) surface has been interpreted as arising from a low proton affinity of the nucleophilic up-dimer atoms of the Ge surface.[38] The higher an activation barrier the reaction has, the harder it is activated. However, at room temperature, this reaction can still proceed to the more stable, dissociated product. This is due to the fact that the activation barrier at room temperature is still surmountable for a low percentage of absorbed water molecules, whereas at lower temperatures, it would be become much more difficult. Kuhr and Ranke[39] found that water adsorbed molecularly without dissociation at 110 K by photoelectron spectroscopy, but annealing the surface at temperatures between 140 and 300 K caused the dissociation of the water molecule. At room temperature, because of the higher activation barrier of dissociation, water molecules adsorbed on Ge(100) may prefer to desorb rather than to dissociate. Therefore, consistent with this, we did observe frequent desorption of SODs from the Ge(100) surface.

To check whether the transformation of SODs to DODs was induced by the STM tip, we scanned the same region several times and then compared the population of DODs on the scanned region with that on an unscanned region. The populations of DODs on the scanned and unscanned areas were almost the same, suggesting that this transformation is not induced by the tip.

Conclusion

We used STM and DFT calculations to study the structure of H_2O adsorbed on Ge(100). We found that H_2O datively bonds via the lone pair electrons on the oxygen atom to the electrophilic down-Ge atom of a buckled dimer on Ge(100), and also dissociatively adsorbs to form Ge−H and Ge−OH species on Ge(100). In addition, we found that, at room temperature, some of the datively bonded adsorbed H_2O molecules (SOD) underwent O−H dissociation to form the H−Ge−Ge−OH dimer, while others were desorbed from the surface. We also observed the structural transformation of SODs to DODs during real-time STM measurements.

Acknowledgment. This research was supported by the Brain Korea 21 Project, the SRC program (Center for Nanotubes and Nanostructured Composites) of MOST/KOSEF, the National R&D Project for Nano Science and Technology, and Grants for Basic Research from the Korea Research Foundation. The calculations were supported by the KISTI through the Seventh Strategic Supercomputing Support Program.

References and Notes

(1) Massoud, H. Z.; Poindexter, E. H.; Helms, C. R. Proceedings of the 1st−3rd International Symposium on the Physics and Chemistry of SiO_2 and the Si/SiO_2 Interface; Electrochemical Society: Pennington, NJ, 1988−1996; Vol. 3.

(2) Horie, T.; Takakuwa, Y.; Miyamoto, N. *Jpn. J. Appl. Phys*. **1994**, *33*, 4684.

(3) Sano, N.; Sekiya, M.; Hara, M.; Kohno, A.; Sameshima, T. *Appl. Phys. Lett*. **1995**, *66*, 2107.

(4) Dujardin, G.; Mayne, A.; Comtet, G.; Hellner, L.; Jamet, M.; Goff, E. L.; Millet, P. *Phys. Rev. Lett*. **1985**, *76*, 3782.

(5) Okamoto, Y. *Phys. Rev. B* **1998**, *58*, 6760.

(6) Niwano, M.; Terashi, M.; Shinohara, M.; Shoji, D.; Miyamoto, N. *Surf. Sci*. **1998**, *401*, 364.

(7) Sneh, O.; Wise, M. L.; Ott, A. W.; Okada, L. A.; George, S. M. *Surf. Sci*. **1995**, 334, 135.

(8) Self, K. W.; Yan, C.; Weinberg, W. H. *Surf. Sci.* **1997**, *380*, 408.

(9) Weldon, M. K.; Stefanov, B. B.; Raghavachari, K.; Chabal, Y. J. *Phys. Rev. Lett*. **1997**, *79*, 2851.

(10) Stefanov, B. B.; Alejandra, B. G.; Makcus, K. W.; Raghavachari, K.; Chabal, Y. J. *Phys. Rev. Lett*. **1998**, *81*, 3908.

(11) Okano, S.; Oshiyama, A. *Surf. Sci*. **2004**, *554*, 272.

(12) Hossain, M. Z.; Yamashita, Y.; Mukai, K.; Yoshinobu, J. *Phys. Rev. B* **2003**, *67*, 153307.
(13) Cho, J.-H.; Kim, K. S.; Lee, S. H.; Kang, M. H. *Phys. Rev. B* **2002**, *61*, 4503.
(14) Konecey, R.; Doren, D. J. *J. Chem. Phys.* **1997**, *106*, 2426.
(15) Chander, M.; Li, Y. Z.; Patrin, J. C.; Weaver, J. H. *Phys. Rev. B* **1993**, *48*, 2493.
(16) Chabal, Y. J. *Phys. Rev. B* **1984**, *29*, 3677.
(17) Chabal, Y. J.; Christman, S. B. *Phys. Rev. B* **1984**, *29*, 6974.
(18) Alejandra, B. G.; Stefanov, B. B.; Makcus, K. W.; Chabal, Y. J.; Raghavachari, K. *Phys. Rev. B* **1998**, *58*, 13434.
(19) Kuhr, H. J.; Ranke, W. *Surf. Sci.* **1987**, *189/190*, 420.
(20) Mui, C.; Senosiain, J. P.; Musgrave, C. B. *Langmuir* **2004**, *20*, 7604.
(21) Föraker, A.; Doren, D. J. *J. Phys. Chem. B* **2003**, *107*, 8507.
(22) Cho, J.-H.; Kleinman, L.; Jin, K.; Kim, K. S. *Phys. Rev. B* **2002**, *66*, 113306.
(23) Chone, S. M.; Yang, Y. L.; Rouchouze, E.; Jin, T.; D'Evelyn, M. P. *J. Vac. Sci. Technol., A* **1992**, *10*, 2166.
(24) Papagno, L.; Caputi, L. S.; Anderson, J.; Lapeyre, G. J. *Phys. Rev. B* **1989**, *40*, 8443.
(25) Larsson, C. U. S.; Flodström, A. S. *Phys. Rev. B* **1991**, *43*, 9281.
(26) Kresse, G.; Furthmüller, J. *Comput. Mater. Sci.* **1996**, *6*, 15.
(27) Kresse, G.; Hafner, J. *J. Phys.: Condens. Matter* **1994**, *6*, 8245.
(28) Tersoff, J.; Hamann, D. R. *Phys. Rev. Lett.* **1983**, *50*, 1998; *Phys. Rev. B* **1985**, *31*, 805.
(29) Cho, Y. E.; Maeng, J. Y.; Kim, S.; Hong, S. *J. Am. Chem. Soc.* **2003**, *125*, 7514.
(30) Krüger, P.; Pollmann, J. *Phys. Rev. Lett.* **1995**, *74*, 1155.
(31) Needels, M.; Payne, M. C.; Joannopoulos, J. D. *Phys. Rev. Lett.* **1987**, *58*, 1765.
(32) Mulcahy, C. P. A.; Carman, A. J.; Casey, S. M. *Surf. Sci.* **2000**, *459*, 1.
(33) Cao, X. P.; Coulter, S. K.; Ellison, M. D.; Liu, J. M.; Hamers, R. J. *J. Phys. Chem. B* **2001**, *105*, 3759.
(34) Wang, G. T.; Mui, C.; Musgrave, C. B.; Bent, S. F. *J. Phys. Chem. B* **2001**, *105*, 3295.
(35) Mui, C.; Wang, G. T.; Bent, S. F.; Musgrave, C. B. *J. Chem. Phys.* **2001**, *114*, 10170.
(36) Luo, H. B.; Lin, M. C. *Chem. Phys. Lett.* **2001**, *343*, 219.
(37) Cao, X. P.; Hamer, R. J. *J. Am. Chem. Soc.* **2001**, *123*, 10988.
(38) Mui, C.; Han, J. H.; Wang, G. T.; Musgrave, C. B.; Bent, S. F. *J. Am. Chem. Soc.* **2002**, *124*, 4027.
(39) Kuhr, H. J.; Ranke, W. *Surf. Sci.* **1987**, *187*, 98.